A numerical study of multi filament formation in metal-ion based CBRAM

Dan Berco and Tseung-Yuen Tseng

Citation: AIP Advances **6**, 025212 (2016); doi: 10.1063/1.4942209
View online: http://dx.doi.org/10.1063/1.4942209
View Table of Contents: http://aip.scitation.org/toc/adv/6/2
Published by the American Institute of Physics

HAVE YOU HEARD?
Employers hiring scientists and engineers trust
PHYSICS TODAY | JOBS
www.physicstoday.org/jobs

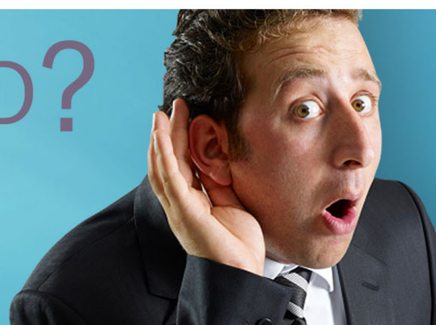

AIP ADVANCES **6**, 025212 (2016)

A numerical study of multi filament formation in metal-ion based CBRAM

Dan Berco[a] and Tseung-Yuen Tseng[b]
Department of Electronics Engineering and Institute of Electronics, National Chiao Tung University, Hsinchu 300, Taiwan

(Received 2 December 2015; accepted 3 February 2016; published online 12 February 2016)

This study investigates the underlying mechanisms of multiple conductive filaments (CF) creation in metal-ion based conductive bridge RRAM (CBRAM) by using the Metropolis Monte Carlo algorithm and suggests a possible explanation for this phenomenon. The simulation method is demonstrated over a Cu/HfO_2 structure, starting from a random initial distribution of oxygen vacancies (OV) defects in the resistive switching layer, to a formed CF and ending in a ruptured state. the results indicate that "Hot Spots" (HS), where agglomeration of OV trap like states for electron hopping based conduction induce local heating, create favorable energy conditions to attract diffused metal species originating from the top electrode. While HS may be created and annihilated by random OV generation and recombination processes, the precipitated metal forms a stem out of which a CF could evolve. The CF stem's final growth stage is mainly driven by drift and diffusion. This process may lead to the formation of one or more CFs as a function of the forming bias voltage. This bias dependence is demonstrated over a large range, where the creation of a single, double and multiple CFs are shown. In addition, the reset process of the multi CF device is presented, and the experimentally observed, step like, gradual CBRAM reset is verified. The simulated results are in good agreement with experimental data and promote the idea that OV defect engineering may be used to improve CBRAM performance. © *2016 Author(s). All article content, except where otherwise noted, is licensed under a Creative Commons Attribution (CC BY) license (http://creativecommons.org/licenses/by/4.0/).* [http://dx.doi.org/10.1063/1.4942209]

INTRODUCTION

Resistive random access memory (RRAM) has attracted great attention due to its potential for the possible replacement of flash memory in next-generation nonvolatile memory (NVM) applications.[1] The conduction mechanism of the oxygen ion-based O-RRAM is due to the formation and rupture of a percolation like conduction path, commonly referred to as a conductive filament (CF), consisting of trap like oxygen vacancies (marked OV with a spatial density N_{ov}) and mobile oxygen species (marked O with a spatial density N_o).[2] Alternatively, the conduction mechanism of the metal-ion based conductive bridging RRAM (CBRAM) make it a favorable candidate for future NVM devices due to fast switching, high endurance and scalability. CBRAM operation is based on the formation and rupture of either Cu or Ag CF in the resistive switching layer (RSL)[3] in addition to the OV where metal oxides are used.

A CBRAM having multiple CFs has been demonstrated experimentally in various structures.[4,5] However, common kinetic based modeling methods,[6,7] that rely on the oxidation and reduction (redox) of metal species by thermal and electro-chemical reactions, mostly address the single CF case. In this work we investigate the phenomena of multi CF creation as a function of the forming voltage bias (V_f) by using the Metropolis Monte Carlo (MMC) algorithm with Gibbs free energy

[a]danny.barkan@gmail.com
[b]tseng@cc.nctu.edu.tw

 ©Author(s) 2016.

(GFE) criteria. The algorithm used in this work is detailed in our previous papers.[8,9] We thus briefly discuss the key aspects of the model in reference to the obtained results. For further information the reader is advised to consult those publications.

MODELING

We demonstrate our approach on a monoclinic hafnium oxide (HfO_2) based metal-insulator-metal (MIM) device and simulate both the forming and reset operation modes, where a CF is formed and ruptured respectively. The RSL is modeled using a 2D rectangular structure, having width W and height H, while divided into a uniform grid (of $\delta = 0.5$ nm spacing). This grid spacing was chosen to be consistent with the typical dimensions of the monoclinic HfO_2 unit cell. Each grid site $n \in N$ is represented by its spatial coordinates (x, y) on which the local potential φ_n, temperature T_n, $N_{o,n}$, $N_{ov,n}$ and electric conductivity σ_n are calculated. The dimensions of the RSL are chosen as W=20 nm and H=10 nm. The top and bottom control electrodes (TE and BE) are located at y=H and y=0 respectively. The BE comprising material (Pt) is considered as inert and the TE material (Cu) acts as the source of metallic species migrating into the RSL (marked Cu with a spatial density $N_{cu,n}$). The RSL temperature is initialized to 297 K and solved using periodic boundary conditions for x=0 and x=W. The initial condition is chosen as room temperature to provide a common consistent reference point with previously published theoretical and experimental results. The values of the parameters used in the simulation, as well as the modeling considerations are elaborated in our previous publications[8,9] and in Ref. 10 and are listed in Table I.

FORMULATION

The Arrhenius model is used to determine the local electrical conductivity over all the grid points $\forall n \in N$ according to:

$$\begin{aligned} \sigma_n &= \sigma_0 \exp(-\frac{E_{ac}}{k_B T_n}) \\ \sigma_0 &= e\frac{eD_0}{k_B T_n} N_{ov} \end{aligned} \tag{1}$$

K_B is Boltzmann's constant, e the electron charge, D_0 the ion diffusivity factor. E_{ac} is the activation energy and σ_0 the pre-exponential conductance.

In the MMC method the simulation starts from an initial configuration and progresses to a pre-determined final configuration in steps, by either accepting or rejecting permutations in the OV density (N_{ov}) at each step, according to the leading minimal energy criteria (GFE). In order to determine the temperature, potential and conduction the charge continuity and steady-state Fourier equations are solved in a self consistent manner. Since N_{ov} is evaluated through the local conductivity, we add the Poisson equation to account for accumulations of O species by the charge density

TABLE I. Parameter values used in this work.

Symbol	Description	Value
f_o	O, Cu ion vibration frequency	10^{13} Hz
Z	O ion charge number	2
E_{ac}	Conductance activation energy	50 meV
D_o	O ion diffusivity factor	2m cm^2/sec
E_o	Cu oxidation activation energy	3.1 eV
E_r	Cu reduction activation energy	3.1 eV
E_{chf}	Cu-HfO2 insertion activation energy	1.3 eV
E_{cov}	Cu-OV insertion activation energy	~0 eV
E_h	O ion hopping barrier	1 eV
a_a	field lowering factor	0.75 nm

$\rho_n = -eZN_o$ (Z is the O ion charge number and ε the RSL permittivity):

$$\begin{aligned} \nabla \cdot \sigma_n \nabla \varphi_n &= 0 \\ \nabla^2 \varphi_n &= \rho_n / \varepsilon \\ -\nabla \cdot k_{th,\,n} \nabla T_n &= \sigma_n |\nabla \varphi_n|^2 \end{aligned} \tag{2}$$

The change in N_o is given by the drift diffusion relation:

$$\begin{aligned} \Delta N_{o,\,n} &= \frac{1}{f_o} \nabla \cdot (D_n \nabla N_{o,\,n} - \frac{eD_n}{k_B T_n} \nabla \varphi_n N_{o,\,n}) \\ D_n &= D_0 \exp(-\frac{E_h}{k_B T_n}) \end{aligned} \tag{3}$$

f_o is the vibrational frequency of the O ion. The material dependent values of the O ion diffusivity factor D_0 and diffusion activation energy E_h are listed in Table I.

The Cu ion oxidation and reduction probabilities are calculated according to:

$$P_n^{o,\,r} = \exp(-\frac{E_{o,\,r} \pm \frac{1}{2}(a_a e \xi_n + \Delta\phi_{RSL-M})}{k_B T_n}) \tag{4}$$

a_a is the field lowering factor for generation, ξ_n is the local electric field, $\Delta\phi_{RSL-M}$ represents the RSL-TE work function difference and $E_{o,\,r}$ the activation energy for Cu oxidation and reduction respectively.

RESULTS

The evolution of a CF involves generation, recombination and hopping of O and OV, which take place on the grid points,[8] in addition to the migration of TE supplied Cu ions. The existence of an OV on a grid site yields favorable energy conditions for the migration of Cu.[9,11,12] The simulation results indicate that, "Hot Spots" (HS)[8] created during the early forming stages within the RSL, serve as agglomeration centers attracting Cu ions to form an initial stem, out of which a CF may evolve, that grows from the TE toward the HS (as illustrated in Figure 1). Although HS may be created and annihilated by the above mentioned random processes, the associated stem remains intact. The creation of a new HS may trigger the sprouting of additional stems, while the growth of existing ones are driven by drift and diffusion forces. In this manner, either a single or multiple CFs

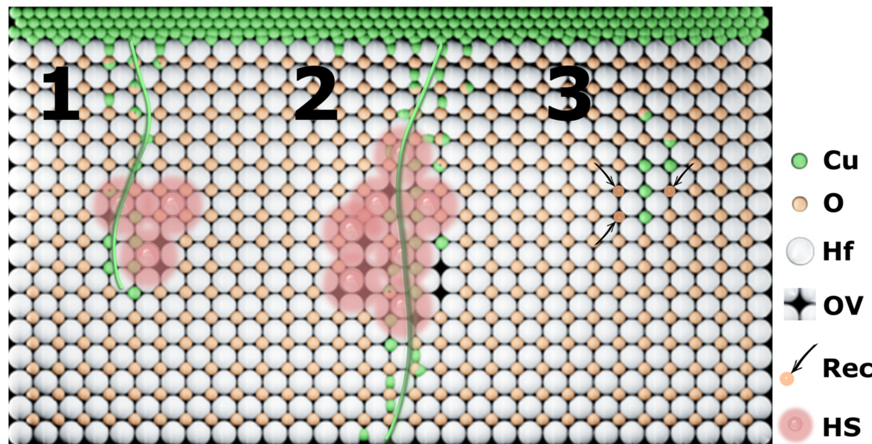

FIG. 1. Schematic illustration of the dominant mechanisms as discussed in this work. (1) formation of a partial CF (marked by a green line representing the formation of a path by the individual Cu) triggered by the presence of a HS (2) formation of a full CF, initiated by the presence of a HS and further driven by a high voltage gradient (3) recombined O-OV reduced the local current and HS temperature leading to a halt in the CF formation.

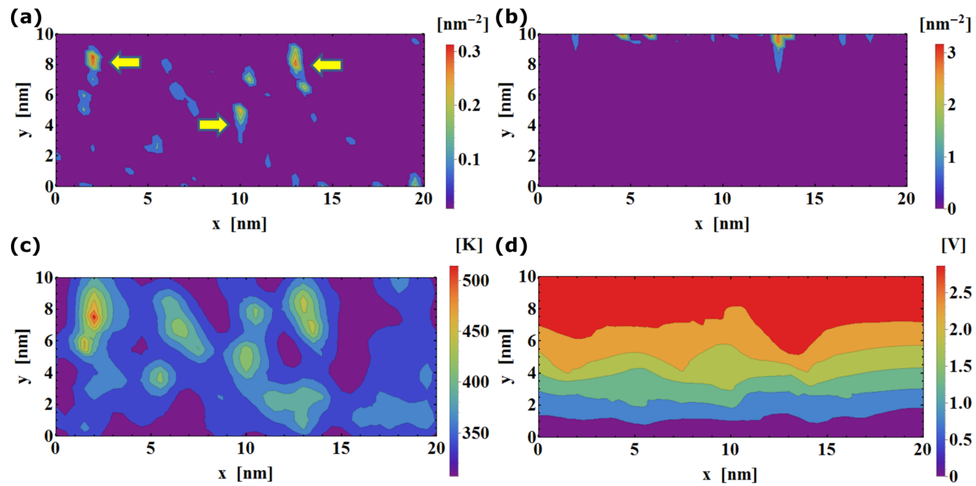

FIG. 2. Initial simulation stages of forming, Vf = 2.95 V, yielding a single CF (hot spots marked with a yellow arrow): (a) N_{ov} (b) N_{cu} (c) Temperature (d) Potential.

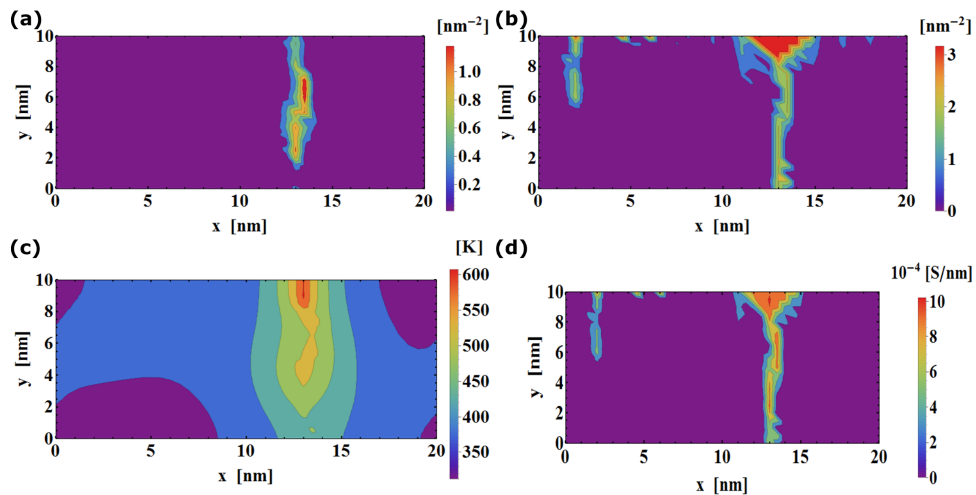

FIG. 3. Final simulation stages of forming, Vf = 2.95 V, yielding a single CF: (a) N_{ov} (b) N_{cu} (c) Temperature (d) Total conductance.

may be created as a function of both V_f and the initial random OV distribution. The CF dependence on the OV random initial distribution was discussed in Ref. 8.

Figure 2 depicts the early simulation stages during forming for $V_f = 2.95$ V. The HS are marked with a yellow arrow in Figure 2(a), while the Cu stems are shown in Figure 2(b). The associated localized high temperature surge is displayed in Figure 2(c) and the RSL potential distribution can be seen in Figure 2(d). HSs located in closer proximity to the TE attract more Cu ions and thus yield larger stems. In this particular case a single HS was dominant, did not annihilate and grew in size toward the TE by added OV.

The 'formed' criterion is defined to be at an overall device current of 1 mA in a similar manner to the current compliance (CC) mechanism used in experimental setups. The current calculations method is detailed in Ref. 8 as well. The resulting single CF is shown in Figure 3 along with the associated temperature profile and total conductance which result in a low resistance state (LRS) value of ∼3 KΩ.

Figure 4 depicts the early simulation stages during forming for $V_f = 4.4$ V. Two dominant HS which were created and sustained throughout the simulation allowed for the formation of two CFs.

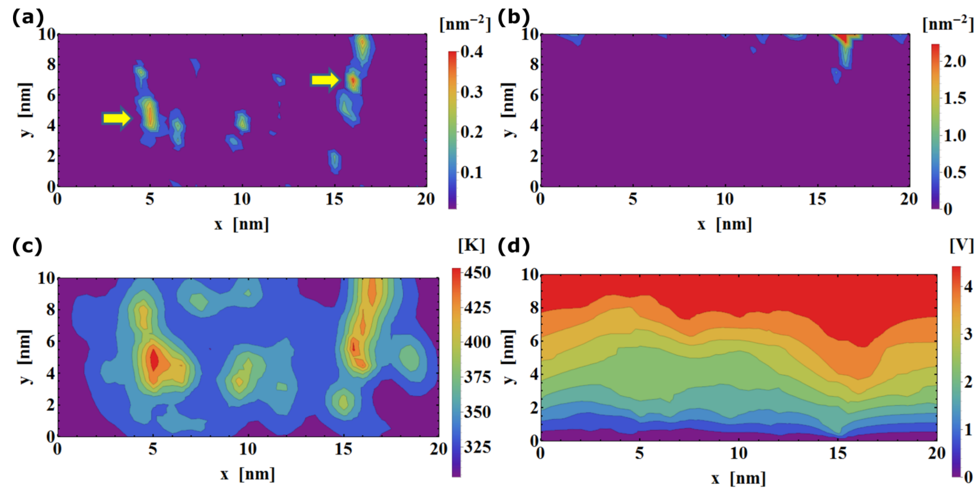

FIG. 4. Initial simulation stages of forming, Vf = 4.4 V, yielding two CFs (hot spots marked with a yellow arrow): (a) N_{ov} (b) N_{cu} (c) Temperature (d) Potential.

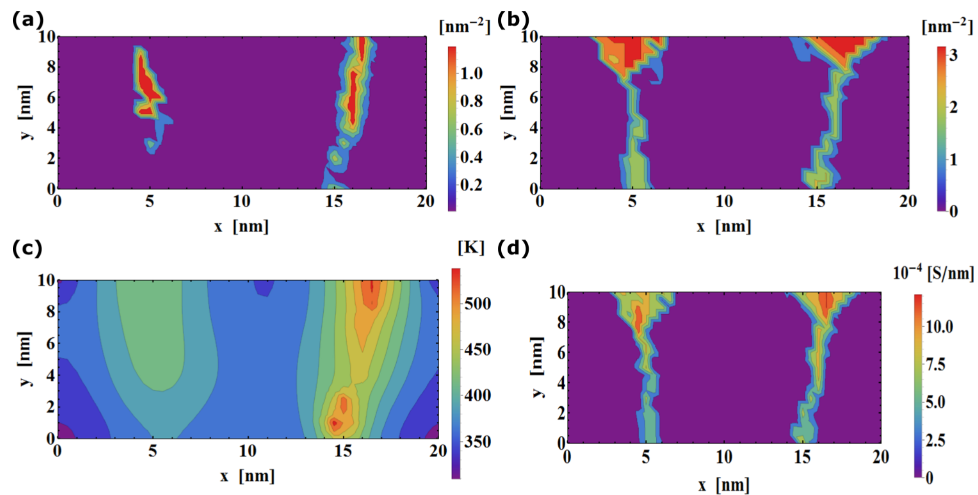

FIG. 5. Final simulation stages of forming, Vf = 4.4 V, yielding two CFs: (a) N_{ov} (b) N_{cu} (c) Temperature (d) Total conductance.

The CC was set to 2.5 mA and the resulting CFs are shown in Figure 5, with a total LRS resistance of ~1.75KΩ.

Figure 6, Figure 7 and Figure 8 show the initial, intermediate and final simulation stages for V_f = 5.2 V forming respectively, with a CC of 5.5 mA. The combination of a large bias along with the temperature profile (Figure 6(c), Figure 7(c)) lead to the annihilation of the early stage HS (Figure 6(a)) and the creation of new HS (Figure 7(a)). The growth of the associated Cu stems, which was initiated by the first HS (Figure 6(b)) up to the intermediate stage (Figure 7(b)), was driven by the high temperature profile (Figure 7(c)) and potential gradient (Figure 7(d)) during the final stages, resulting in multiple CFs (Figure 8(b), 8(d)) and an overall LRS resistance of roughly 900 Ω.

The RSL properties for the 'reset' final simulation stages of the multi CF case (Figure 8) are displayed in Figure 9. The reset potential (V_r) is set to $V_r = -1.55$ V and the device is considered as 'reset' once all CF are ruptured (Figure 9(b)). The resulting high potential gradients at the tips of the CF (Figure 9(d)) are the main driving mechanism for the reforming of a CF during the 'set' operation mode as discussed in Ref. 8.

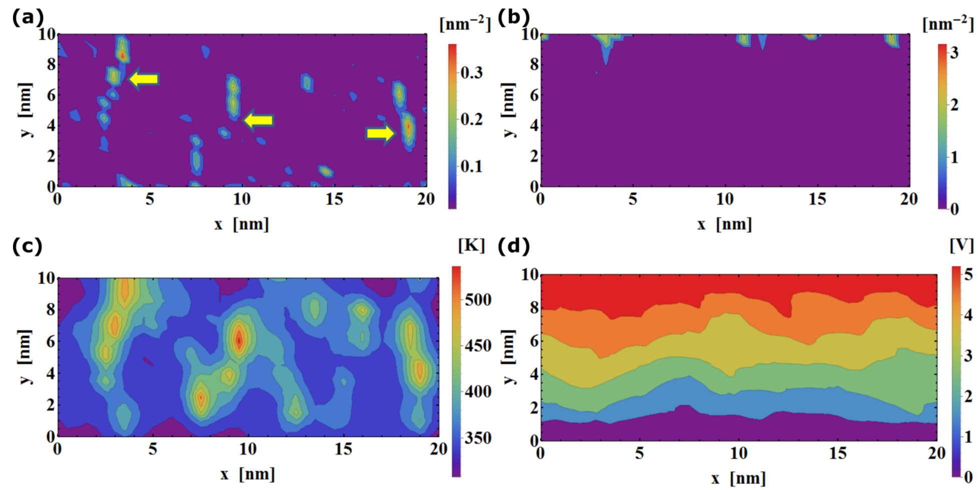

FIG. 6. Initial simulation stages of forming, Vf = 5.2 V, yielding multiple CFs (hot spots marked with a yellow arrow): (a) N_{ov} (b) N_{cu} (c) Temperature (d) Potential.

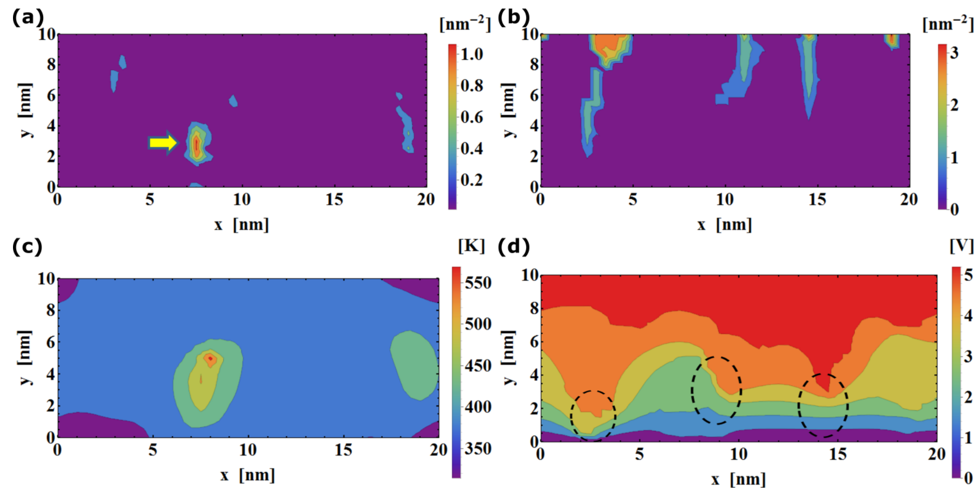

FIG. 7. Intermediate simulation stages of forming, Vf = 5.2 V, yielding multiple CFs (hot spots marked with a yellow arrow): (a) N_{ov} (b) N_{cu} (c) Temperature (d) Potential (large gradient areas marked with a dashed circle).

The dependence of the 'forming' current on V_f is shown in Figure 10(a). The figure contains both gradually increasing sections, where a larger V_f is manifested in CF thickening, and abrupt transitions, where multiple CFs are formed. Figure 10(b) depicts the total current during 'reset' as a function of the simulation step count. The progressive nature of this operation mode is evident, where step like current drops occur whenever a CF is ruptured, thus supporting experimental observations of the CBRAM progressive reset phenomena.[13–15] Figure 11 (Multimedia view) shows the simulation progress for the discussed CF cases and is provided for illustrative purposes.

The published work by Tsai *et al.*[13] details the experimental results for a CBRAM device having a similar structure with respect to both size and composition to the one simulated in this paper. Annealing in O_2 atmosphere, as done by Tsai, is believed to considerably reduce the number of OV defects in the HfO_2RSL when compared to the vacuum counterpart. This lower amount of OV may be viewed as a low initial RSL disorder.[8,9] Furthermore, although a rich OV RSL results in poor performance and high leakage in OxRRAM devices, it can help to improve CBRAM characteristics by facilitating a consistent CF structure. This notion is demonstrated in this manuscript by the role of HS in CF formation and was also verified in Ref. 9. The idea of defect engineering (one might imagine a fault line throughout the RSL composed of aligned grain boundaries from TE to BE) may

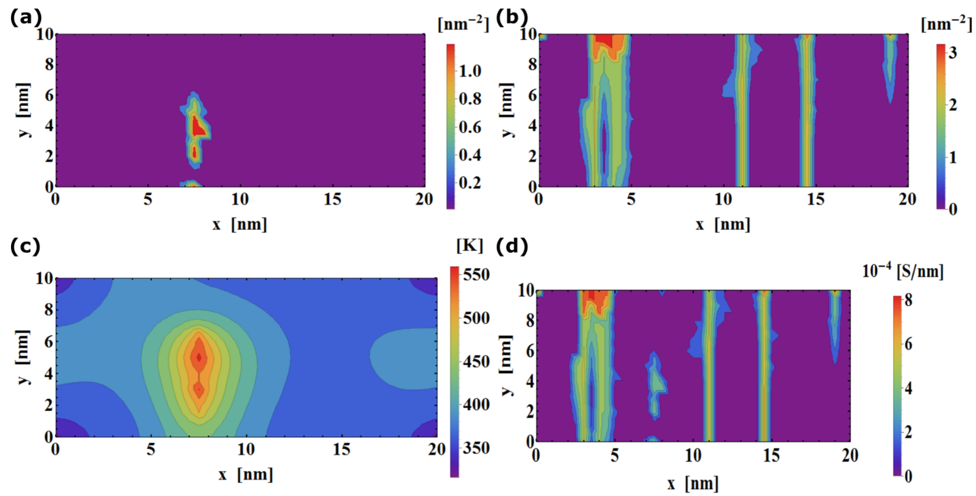

FIG. 8. Final simulation stages of forming, Vf = 5.2 V, yielding multiple CFs: (a) N_{ov} (b) N_{cu} (c) Temperature (d) Potential.

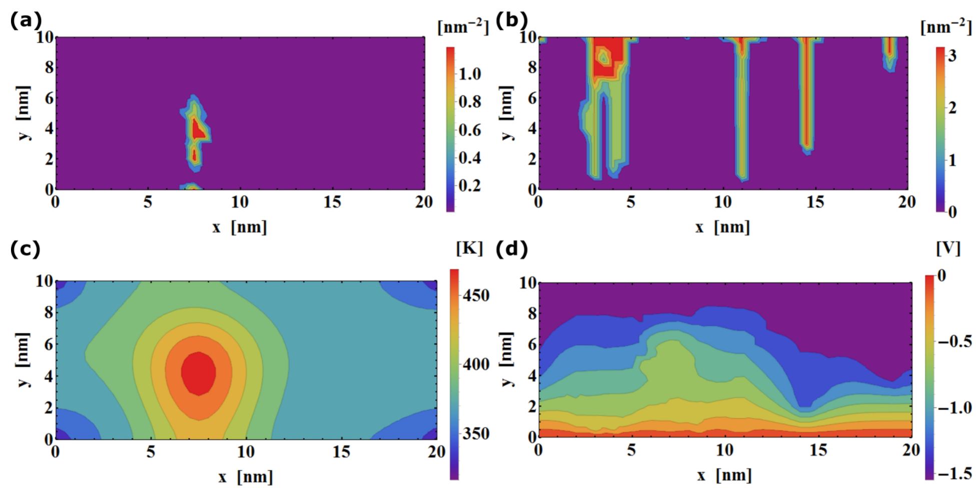

FIG. 9. Final simulation stages of rupture in the multiple CFs case, Vr = −1.55 V: (a) N_{ov} (b) N_{cu} (c) Temperature (d) Potential.

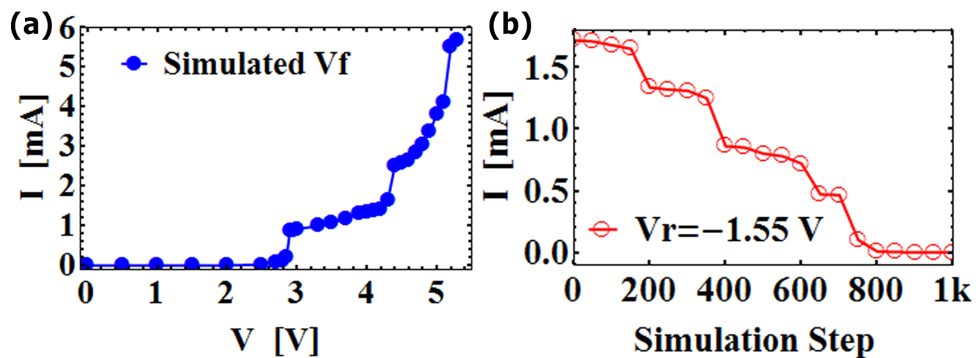

FIG. 10. (a) Forming: total device current dependence on forming voltage indicating the abrupt transition points (2.95, 4.4 and 5.2 V) where a CF formation occurred (b) Reset: current dependence on the simulation step count indicating the step like transitions where individual CFs have been ruptured.

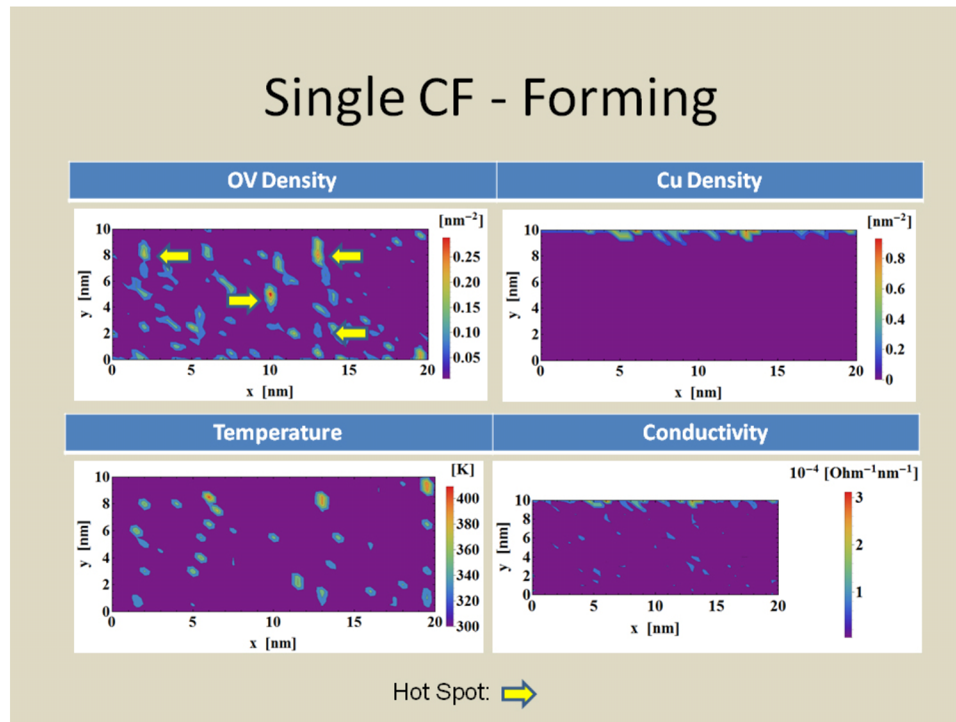

FIG. 11. Simulation progress for the various CF cases presented in this work. (Multimedia view) [URL: http://dx.doi.org/10.1063/1.4942209.1]

help to greatly reduce the statistical distribution of device characteristics by yielding a more regular CF, in a similar manner to the demonstrated existence of a single dominant HS, having a large initial OV concentration gradient that resulted in a single CF.

Our result for $V_f = 2.95$ V matches the one of the 400 °C O_2 device by Tsai (ranged between 2-3 V), which may indicate a match of the RSL disorder level, taken in our simulations as 0.3 nm^{-3}, to this process. As for device reset, the physical mechanisms that determine V_r are much less dependent on the initial RSL state as elaborated in Ref. 8 and seen in the experimental data by Tsai. The measured variance of V_r by Tsai is between ∼1.2-1.5 V, with an average of ∼1.4 V for the 400 °C annealed devices, and between ∼ 1.1-1.4 V, with an average of ∼1.3 V for the 500 °C annealed devices. Our simulated result of $V_r = -1.55$ V is not far from this range and falls within the overall distribution of the data by Tsai (ranged between 0.9-1.7 V). In addition, the LRS resistance of ∼3 KΩ for a single CF, as presented in this work, is compatible to the measured one that shows a stable retention level of ∼1.2 KΩ for 400 °C annealed CBRAM, when accounting for the double RSL thickness as used in our model.

Our results are also consistent with published experimental data with respect to the CF growth kinetics, being directed from the anode to the cathode,[4,5] as well as composition,[14] containing both Cu and OV, and where the sequential or simultaneous rupture of heterogonous CF are used to explain progressive reset phenomena (also demonstrated by our previous work[9]). In addition, our calculated values for V_f and V_r are consistent with,[14,16] and the LRS resistance is within the range measured by Lin *et al.*[17] (∼5K for a 50 nm RSL) and Xu *et al.*[18] (∼1K for a 4 nm RSL) for the single CF case. Furthermore, a quick estimation reveals that the parallel conductance of two (Figure 5(d)) and four CFs (Figure 8(d)) is also consistent with this range.

CONCLUSIONS

We investigate the mechanisms for creation of multiple CFs in metal-ion based CBRAM. Our results indicate that HSs generate favorable conditions to attract diffused metal ions from the TE.

As HSs are created, the precipitated ions form a stem out of which one or more CFs may evolve as a function of V_f. In addition, the reset of the multi CF device is shown to have a step like, gradual transition as the CFs are ruptured sequentially. Based on the presented results, we promote the idea of RSL defect engineering. While the notion of deliberate introduction of OV into the RSL during fabrication may prove to be devastating in the O-RRAM case, it may help to control the structure and number of CF in a CBRAM device, thus considerably improving its performance, as also demonstrated by Tsai *et al.*[13]

ACKNOWLEDGMENTS

This work is supported by Ministry of Science and Technology, Taiwan, under Project No. NSC 102-2221-E-009-134-MY3.

[1] T. Y. Tseng and S. M. Sze, Am. Scientific Pub., CA. USA, ,Vol. 1, p.1 (2012).
[2] H.-S. P. Wong, H. Y. Lee, S. Yu, Y. S. Chen, Y. Wu, P. S. Chen, B. Lee, F. T. Chen, and M. J. Tsai, Proc. IEEE **100**(6), 1951–1970 (2012).
[3] U. Russo, D. Kamalanathan, D. Ielmini, A. L. Lacaita, and M. N. Kozicki, Trans on Elec. Dev. **56**(5), 1040–1047 (2009).
[4] X. Wu, K. Li, N. Raghavan, M. Bosman, Q.-X. Wang, D. Cha, X.-X. Zhang, and K.-L. Pey, Appl. Phy. Lett. **99**, 093502 (2011).
[5] J. Sun, X. Wu, Q. Liu, and M. Liu, in *20th IEEE International Symposium (IPFA)*, pp. 560–562 (July 2013), DOI: 10.1109/IPFA.2013.6599223.
[6] F. Pan, S. Yin, and V. Subramanian, Electron. Dev. Lett. **32**(7), (July 2011).
[7] S. Qin, Z. Liu, G. Zhang, J. Zhang, Y. Sun, H. Wu, H. Qian, and Z. Yu, Phys. Chem. Chem Phys. **17**(14), (2015).
[8] D. Berco and T. Y. Tseng, Journal of Computational Electronics (August 2015), DOI: 10.1007/s10825-015-0736-7.
[9] D. Berco and T. Y. Tseng, Journal of Computational Electronics (August 2015), DOI: 10.1007/s10825-015-0744-7.
[10] W. M. Haynes, *CRC Handbook of Chemistry and Physics*, 91st ed. (CRC press, Boca Raton, FL, 2010), pp. 5-16–5-17.
[11] J. Guy, G. Molas, P. Blaise, C. Carabasse, M. Bernard, A. Roule, G. Le Carval, V. Sousa, H. Grampeix, V. Delaye, A. Toffoli, J. Cluzel, P. Brianceau, O. Pollet, V. Balan, S. Barraud, O. Cueto, G. Ghibaudo, F. Clermidy, B. De Salvo, and L. Perniola, in *IEDM* (2014), pp. 6.5.1–6.5.4.
[12] G. Molas, E. Vianello, F. Dahmani, M. Barci, P. Blaise, J. Guy, A. Toffoli, M. Bernard, A. Roule, F. Pierre1, C. Licitra, B. De Salvo, and L. Perniola, in *IEDM* (2014), pp. 6.1.1–6.1.4.
[13] T. L. Tsai, H. Y. Chang, F. S. Jiang, and T. Y. Tseng, Electron Dev. Lett. **36**(11), 1146–1148 (2015).
[14] X. L. Shao, J. S. Zhao, K. L. Zhang, R. Chen, K. Sun, C. J. Chen, K. Liu, L. W. Zhou, J. Y. Wang, C. M. Ma, K. J. Yoon, and C. S. Hwang, ACS Appl. Mater. Interfaces **5**(21), 11265–11270 (2013).
[15] U. Celano, L. Goux, A. Belmonte, G. Giammaria, K. Opsomer, C. Detavernier, O. Richard, H. Bender, F. Irrera, M. Jurczak1, and W. Vandervorst, in *IEDM 2014* (2014), pp. 14.1.1–14.1.4.
[16] M. Barci, J. Guy, G. Molas, E. Vianello, A. Toffoli, J. Cluzel, A. Roule, M. Bernard, C. Sabbione, L. Perniola, and B. De Salvo, in *IEEE International Reliability Physics Symposium* (2014), pp. 5E.3.1–5E.3.4 DOI:10.1109/IRPS.2014.6860677.
[17] K.-L. Lin, T.-H. Hou, J. Shieh, J.-H. Lin, C.-T. Chou, and Y.-J. Lee, Jour. Appl. Phy. **109**, 084104 (2011).
[18] X. Xu, H. Lv, H. Liu, T. Gong, G. Wang, M. Zhang, Y. Li, Q. Liu, S. Long, and M. Liu, IEEE Elect. Dev. Lett. **36**(2), (FEBRUARY 2015).